Lunar Pits and Hawaiian Analogs

R. V. Wagner[1], S. K. Rowland[2], M. S. Robinson[1], and the LROC Team
[1]Lunar Reconnaissance Orbiter Camera, School of Earth and Space Exploration, Arizona State University, Tempe, AZ 85287-3603; rvwagner@asu.edu
[2]Department of Geology and Geophysics, University of Hawai'i at Mānoa, Honolulu, HI

Abstract #1538

Introduction

The Lunar Reconnaissance Orbiter Narrow Angle Camera (NAC) consists of two line-scan cameras aimed side-by-side with a combined 5.7° FOV, with a nominal resolution of 0.5 m/px from the original mission altitude of 50 km. To date, over 300 vertical-walled lunar collapse pits have been discovered, all but three from analysis of NAC images [1,2], and recent measurements suggest that some may be associated with large underground void spaces [3,4]. Our previous NAC-based investigations of lunar pits revealed overhung void spaces [2] and meter-scale layering in the walls interpreted as mare flows [5]. Terrestrial pit craters, including several examples in Hawai'i, have been proposed as analogs for lunar and martian pits [2,6]. Here, we analyze NAC observations of lunar pits in the context of new 3D models of Hawaiian pit craters.

Pit Topographic Models

We produced models of three pit craters [7] in Hawai'i Volcanos National Park: Devil's Throat and the Twin Pits. We collected photographs from the pit rims (**Figure 1**) and processed these images with the commercial photogrammetric software Photoscan to produce georeferenced 3D point clouds and triangle meshes (**Figure 2**). These models have a point spacing of ~5 cm, and a relative accuracy between points of ~10 cm [8].

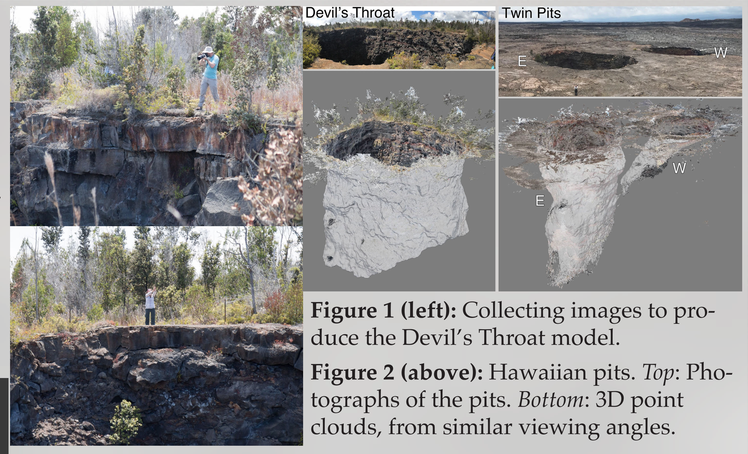

Figure 1 (left): Collecting images to produce the Devil's Throat model.

Figure 2 (above): Hawaiian pits. *Top*: Photographs of the pits. *Bottom*: 3D point clouds, from similar viewing angles.

Creating Synthetic NACs

To compare these terrestrial pit models with the lunar examples, we created images of them with LROC-NAC-like perspectives. To produce these synthetic NAC images, we used the NAIF SPICE data associated with NAC images of pits to determine the camera and Sun postitions and orientations relative to the pit, and reproduced those conditions in Blender using a virtual camera that matched the NAC optical parameters. We then rendered the terrestrial scene, and downsampled the resulting image to match the pixel scale of the lunar image (**Figure 3**).

These synthetic images do not contain any albedo information; we used an untextured model with a close-to-default lighting model (we reduced the default specular intensity to 0.1 for a more matte, Moon-like appearance). Future work may attempt to use desaturated textures derived from the source photographs to add albedo to the synthetic NACs (although the early-afternoon lighting in that texture model will complicate accurate simulation of lighting).

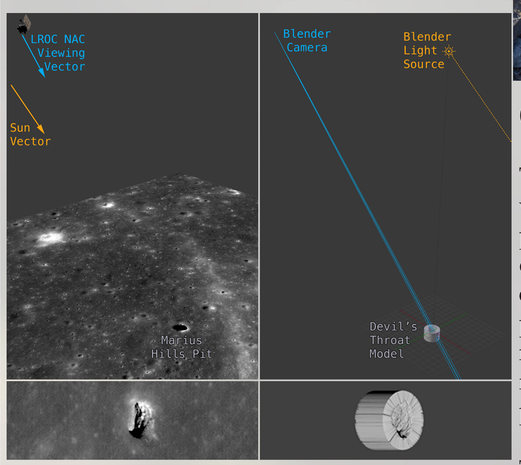

Figure 3: Creation of a synthetic NAC image. *Left*: Geometry of original slewed image (*top*) and actual image M1221699331L (*bottom*). *Right*: Blender scene with matching parameters (*top*), and rendered synthetic NAC view of Devil's Throat (*bottom*). Distances and sizes are not to scale; angles are.

Overhangs and Wall Profiles

We have reconstructed profile lines down the east and west walls of the Mare Tranquillitatis pit using multiple off-nadir observations with similar lighting conditions taken over the course of the LRO mission. Due to the small feature size, inconsistent lighting, and, in the case of the west wall, 2.6x resolution difference between images, we relied on manual point-matching, rather than automated algorithms.

We measured feature positions to the nearest half pixel and assumed a ±1 pixel error in those measurements for uncertainty calculations. We found that a convergence angle of ~20° struck the best balance between uncertainty from measurement errors and easy manual identification of matching points between images.

Figure 4 shows the profiles of the upper ~40 m of the Mare Tranquillitatis pit on both sides, using the apparent start of the vertical wall ("inner rim", per the terminology in [2]) as the reference point for the profiles (dark blue dots). For the east wall, we also show the approximate wall angle derived from illumination conditions in some off-nadir images.

As an accuracy check, we also used this technique on two synthetic NACs of the Devil's Throat pit, and compared the resulting profile to a cross-section of the model used to create those synthetic NACs (**Figure 4**, *right*). The profile points aligned to the original model to within their one-pixel measurement error.

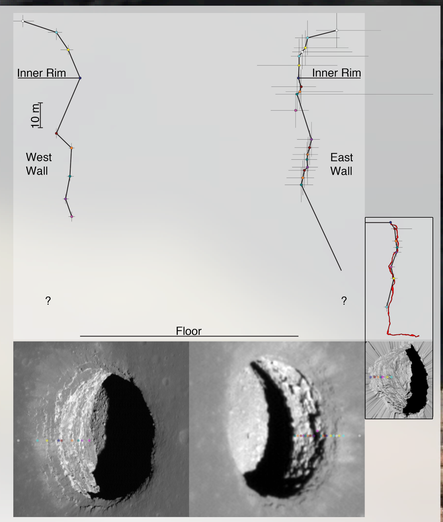

Figure 4: Approximate cross-section of the Mare Tranquillitatis pit wall geometry. Dots mark measured points on the wall, with 1-pixel error bars. Lines are interpolated. *Right*: Cross-section of Devils Throat west wall at the same scale, using the same image geometry as for the west wall of Tranquilitatis. Red line is actual pit model geometry.

Poster in 60 seconds

The Problem: We have limited data on lunar pits: In LROC NAC images, pits are usually < 100 pixels wide.

The Question: Can we use Earth analogs to inform our interpretation of LROC images of lunar pits?

The Method: We produced ~10 cm resolution 3D models of three pit craters in Hawai'i, and used those to create synthetic "LROC NAC" images of those pits.

The Results: We have determined that layer analyses from LROC NAC images of lunar pits likely underestimate the actual number of flow layers in pit walls. Additionally, we can accurately calculate wall profiles from orbital images, given a suitable convergence angle.

Layering Analysis

Shadow and albedo patterns in the walls of lunar mare pits have been interpreted as outcrops of individual flow layers in the maria, with thicknesses ranging 1-13 m ([6], and see **Figure 5**). To test the interpretation of layering (and flows) within the walls of the lunar pits, we used synthetic NAC images of the terrestrial pits to identify morphologically-separated layers. We then compared these layer boundaries to layers identified in high-resolution photographs (~5 mm/px) of the terrestrial pits.

At Devil's Throat, we identified four probable layer boundaries in the synthetic NAC image, as well as the floor-wall boundary (**Figure 6**). Of these, the upper two correspond to identified flow boundaries in the pit wall, while the lower two are below the level (~20 m depth) where flow boundaries can be conclusively identified from our rim photography, but do correspond to overhangs that may be a result of a strength differences between layers (soil or ash layer between flows). In the upper 20 m of the pit wall, there are at least three additional flow boundaries that are not clearly resolved in the synthetic NAC (Figure 6; blue lines). This analysis suggests that number of layers and their thicknesses identified in NAC images of lunar pits [6] is likely a conservative estimate of the actual number of layers.

In the east Twin Pit wall, flow boundary identification is difficult due to an apparent surficial coating below ~10 m depth, possibly related to a post-collapse lava flow (the overhung wall of the west pit shows clear layering (background image), but unfortunately is not visible in synthetic NACs due to the high degree of overhang, visible in **Figure 2**). In the lunar cases, there may be similar effects from post-collapse dust and regolith deposition. In this case, one of the layers from the synthetic NAC does correspond to the only clearly identifiable flow boundary in the ground-level images.

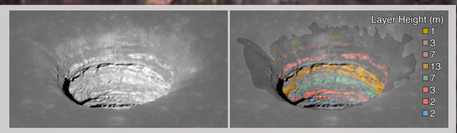

Figure 5: Layers in Mare Tranquillitatis west wall, redrawn following Figure 5 of [5] using higher-resolution base imagery.

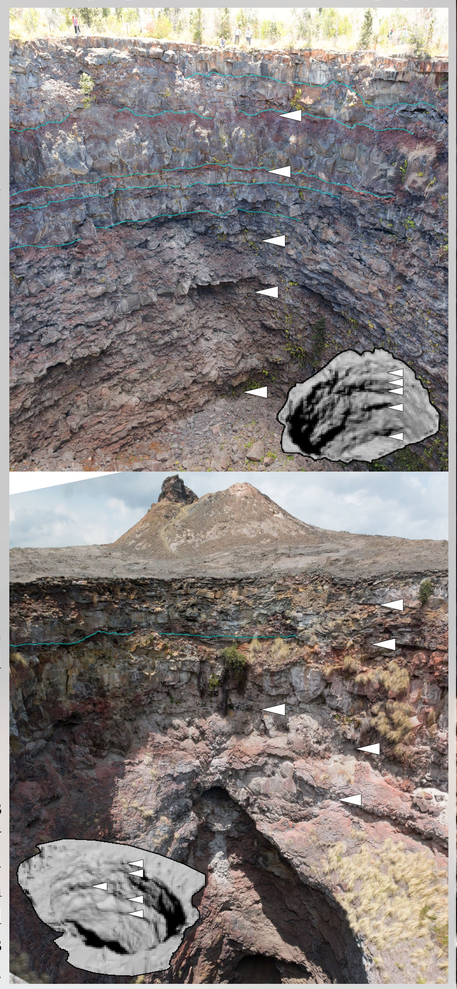

Figure 6: Layering analysis of the west walls of Devil's Throat (*top*; wall is ~47 m high) and east Twin Pit (*bottom*; lowest white arrow is ~24 m below surface). Both panels are mosaics of multiple photographs; at Devil's Throat, we only acquired images with good color of this wall above ~20 m depth (~3rd white arrow) due to safety considerations. Blue lines mark identified flow boundaries (based primarily on reddish oxidized layers); white arrows mark layers identified in the synthetics NACs (*insets*) using shadowing.

References

[1] Haruyama et al. (2010), *41st LPSC*, abstract #1285
[2] Wagner and Robinson (2014), *Icarus*, 237C, 52–60. doi: 10.1016/j.icarus. 2014.04.002
[3] Chappaz et al. (2017) *Geophys. Res. Lett.*, 44, 105-112. doi: 10.1002/2016GL071588
[4] Kaku et al. (2017) *Geophys. Res. Lett.*, 44, 10,155-10,161, doi: 10.1002/2017GL074998.
[5] Robinson et al. (2012), *Planet. and Space Sci.*, 69, 18-27, doi: 10.1016/j.pss.2012.05.008
[6] Cushing et al. (2015) *J. Geophys. Res. Planets*, 120, 1,023-1,043, doi: 10.1002/2014JE004735
[7] Okubo and Martel (1998), *J. Volc. And Geotherm. Res.*, 86, 1-18.
[8] Wagner et al. (2017), *3rd Planet. Data Wkshp.*, abstract #7023

Special thanks to Megan Henriksen, Madeleine Manheim, Emerson Speyerer, and Aaron Boyd of the LROC team for taking many of the ~3300 photographs used in this analysis.

(**Background:** South wall and descending passage of the western Twin Pit, to ~50 meters depth.)

Abstract
Scan this code to view the abstract for this poster.

E-Poster
Scan this code to view this poster online.